Induction Motors Bearing Failures Detection and Diagnosis Using a RBF ANN Park Pattern Based Method

Izzet Önel, Ibrahim Senol, Mohamed Benbouzid

Induction Motors Bearing Failures Detection and Diagnosis Using a RBF ANN Park Pattern Based Method

I. Y. Önel, I. Şenol and M. E. H. Benbouzid

***Abstract*—This paper deals with the problem of bearing failure detection and diagnosis in induction motors. The proposed approach is a sensor-based technique using the mains current and the rotor speed measurement. The proposed approach is based on the stator current Park patterns. Induction motor stator currents are measured, recorded and used for Park patterns computation. A Radial Basis Function (RBF) Artificial Neural Network (ANN) is then used to automate the fault detection and diagnosis process. Experimental tests with artificial bearing damages results show that the proposed method can be used for accurate bearing failures detection and diagnosis in induction motors.**

***Index Terms*—Induction motor, bearing failure, diagnosis, Park transform, neural networks.**

I. Introduction

IN recent years, marked improvement has been achieved in the design and manufacture of stator winding. However, motors driven by solid-state inverters undergo severe voltage stresses due to rapid switch-on and switch-off of semiconductor switches. Also, induction motors are required to operate in highly corrosive and dusty environments. Requirements such as these have spurred the development of vastly improved insulation material and treatment processes. But cage rotor design has undergone little change. As a result, rotor failures now account for a larger percentage of total induction motor failures (Fig. 1) [1-2]. Bearings deterioration is now the main cause of rotor failures.

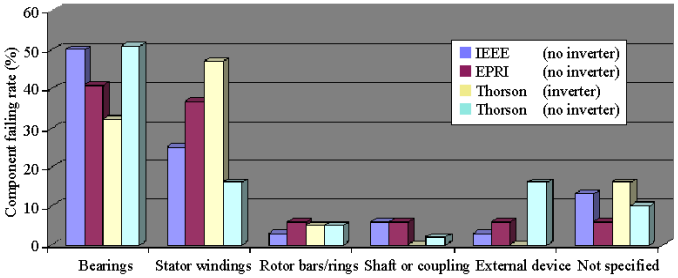

Fig. 1. Induction motor component failing rate versus survey.

Manuscript received June 30, 2006.

I.Y. Önel and I. Şenol are with the Electrical Engineering Department, Electrical-Electronics Faculty, Yildiz Technical University – YTU Merkez Kampus, Istanbul, Turkey (e-mail: senol@yildiz.edu.tr).

M.E.H. Benbouzid is with the Laboratoire d'Ingénierie Mécanique et Electrique (LIME), University of Western Brittany, Rue de Kergoat – BP 93169, 29231 Brest Cedex 3, France (phone: +33 2 98 01 80 07; fax: +33 2 98 01 66 43; e-mail: m.benbouzid@ieee.org).

A. Bearing Failures

There are many reasons to trigger bearing faults. The main factor of bearing faults is dust and corrosion. Induction motors are often operated in hard conditions. That is why foreign materials, water, acid and humidity are the main reasons of bearing deteriorations. Contamination and corrosion frequently accelerate bearing failures because of the harsh environments present in most industrial settings. Dirt and other foreign matter that is commonly present often contaminate the bearing lubrication. The abrasive nature of this minute particles, whose hardness can vary from relatively soft the diamond like, cause pitting and sanding actions that give way to measurable wear of the balls and raceways [3]. Bearing corrosion is produced by the presence of water, acids, deteriorated lubrication and even perspiration from careless handling during installations. Once, the chemical reaction has advanced sufficiently, particles are worn off resulting in the same abrasive action produced by bearing contamination. Improper lubrication includes both under and over lubrication. In either case, the rolling elements are not allowed to rotate on the designed oil film causing increased levels of heating. The excessive heating causes the grease to break down, which reduces its ability to lubricate the bearing elements and accelerates the failure process [3-5].

Bearing problems are also caused by improperly forcing the bearing onto the shaft or into the housing. This produces physical damage in the form of brinelling or false brinelling of the raceways, which leads to premature failure. Misalignment of the bearing, which occurs in the four ways depicted in Fig. 2, is also a common result of defective bearing installation.

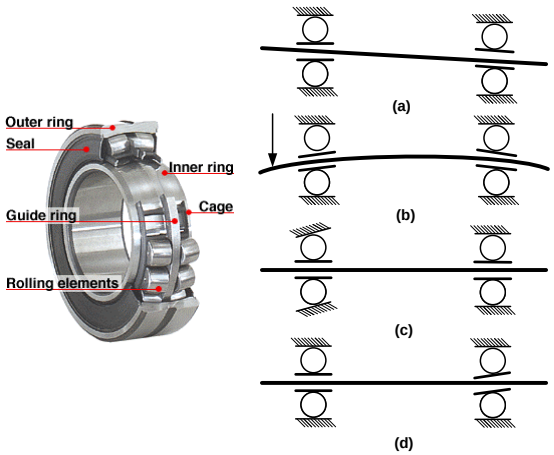

Fig. 2. (a) Misalignment (out-of-line), (b) Shaft deflection, (c) Cocked or tilted outer race, (d) Cocked or tilted inner race.

In a small fraction of induction motor applications, bearings prematurely fail due to electrical causes. Currents flowing through induction motor bearings have the potential of creating premature failure of these bearings. Figure 3 shows the typical fluting pattern in a bearing race due to metallurgical damage from interrupted electrical current flow. Increased noise and vibration are typical symptoms of bearing damage for a bearing such as this. Over time, lubrication fatigue and mechanical wear lead to ultimate bearing failure [6].

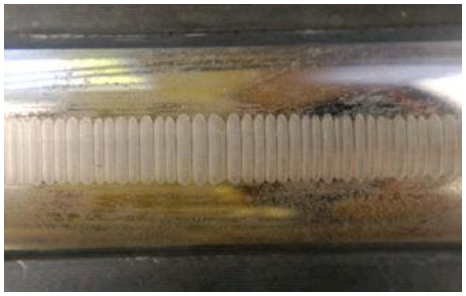

Fig. 3. Bearing fluting.

B. State of The Art

There are many condition monitoring methods used for the detection and the diagnosis of bearing failure: vibration measurements, temperature measurement, shock pulse method (SPM) and acoustic emission (AE). Among these vibration measurements are most widely used [7]. A detailed review of different vibration and acoustic methods, such as vibration measurements in time and frequency domains, sound measurement, the SPM and the AE technique for condition monitoring of bearing failure is given in [8]. In fact, large induction motors are often equipped with mechanical sensors, which are primarily vibration sensors such as proximity probes. However, these are delicate and expensive. Moreover, it is not economically or physically feasible to provide the same for smaller induction motors.

Owing to the infeasibility of these traditional techniques because of the economical constraints in small and medium size induction motors, stator current harmonics measurement is appearing as an alternative to the vibration measurement methods. Indeed, various researchers have suggested that stator current monitoring can provide the same indications without requiring access to the motor. This technique utilises results of spectral analysis of the stator current or supply current of an induction motor for the diagnosis [9-10]. Example techniques that have been also investigated to bearing failure detection and/or diagnosis include statistical methods [11], wavelets [12], and ANN [13].

According to the available literature and with the objective of diagnosing bearing failures in induction motors, without requiring access to the motor, this paper proposes an approach that is based on the stator current Park patterns processing. The global applicability of such an approach has been demonstrated in [14] for induction motor stator faults and in [15] for bearing failures. The originality of the proposed detection and diagnosis rely on the well-processing of the stator currents (using Park patterns associated to the induction motor rotor) and the use of RBF ANN to automate the fault detection and diagnosis process.

II. Park Transform

A two dimensional representation can be used for describing three-phase induction motor phenomena. A suitable one being based on the stator current Park vector [1]. Park transform reduces the number of current components and makes the calculation easier. It should be noted that Park and Concordia transforms are often mingled [16].

In a three-phase induction motor, stator current has three (*a*,*b*,*c*) components. When Concordia transform is applied to the mains, *sD* and *sQ* components of the stator current are obtained. This transform is governed by (1).

$$\begin{cases} I_{sD} = \sqrt{\frac{2}{3}} I_a - \frac{1}{\sqrt{6}} I_b - \frac{1}{\sqrt{6}} I_c \\ I_{sQ} = \frac{1}{\sqrt{2}} I_b - \frac{1}{\sqrt{2}} I_c \end{cases} \quad (1)$$

These components are stationary according to the stator.

If Park transform (2) is applied to the *sD*-*sQ* system, *D* and *Q* components are obtained.

$$\begin{bmatrix} I_D \\ I_Q \end{bmatrix} = \begin{bmatrix} \cos\theta_r & \sin\theta_r \\ -\sin\theta_r & \cos\theta_r \end{bmatrix} \begin{bmatrix} I_{sD} \\ I_{SQ} \end{bmatrix} \quad (2)$$

These components are stationary according to the rotor. Figure 4 summarizes the above transforms where I_s is the stator current vector that rotates at the angular frequency ω_s.

Transforming *abc* system to *sD*-*sQ* system is very simple. Park transform is more complicated than Concordia's. Indeed, rotor speed or position must be known. But stator current *D* and *Q* components have valuable information for bearing fault detection. Indeed, they contain the speed information that is obviously affected by bearings condition.

Using this new Park transform, the obtained *D* and *Q* current trajectory is not a circle, as it is the case for *sD* and *sQ* current trajectory: It is an ellipse as schematically depicted by Fig. 5. It is also a simple reference figure that allows the detection of abnormal conditions by monitoring the deviations of acquired patterns: The occurrence of a bearing failures manifest itself in the deformation of the ellipse.

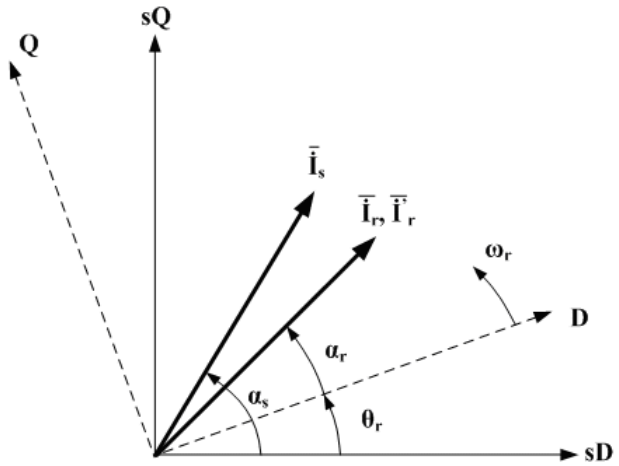

Fig. 4. Representation of *sD*-*sQ* and *D*-*Q* axes.

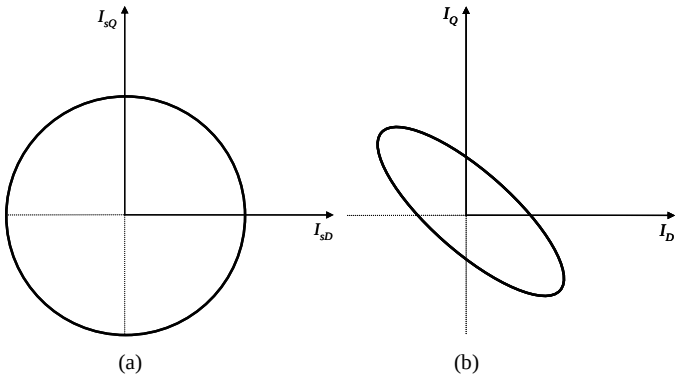

Fig. 5. Current patterns for ideal conditions: (a) Concordia transform. (b) The new Park transform.

III. The RBF Neural Network

A. Why RBF Neural Networks

Recent developments in diagnosis systems have led to extensive use of artificial intelligence (AI) techniques have been proposed for the noninvasive machine fault detection [17-18]. They have several advantages over the traditional model-based techniques. They require no detailed analysis of the different kinds of faults or modeling of the system. These AI-based techniques include expert systems, neural network, and fuzzy logic. Neural network approaches can be considered as "black-box" methods as they do not provide heuristic reasoning about the fault detection process. In this paper ANN are used due to their numerous advantages over conventional diagnosis techniques. In general, when properly tuned, they could improve the diagnosis performance. They are easy to extend and modify, and they could be easily adapted by the incorporation of new data as they became available.

RBF neural networks have been adopted because they are able to provide an accurate fault diagnostic classification. The advantages of using RBF neural networks are twofold. First, the best possible network architecture is determined according to the input data by a well-proposed training algorithm. It does not require the many trial tests to determine the appropriate network architecture. This feature is user friendly for general industrial applications. Second, the outputs of the neural network are able to not only perform fault detection, but also indicate the extent of the fault (diagnosis) [20].

B. The Adopted RBF Neural Network Architecture

The RBF networks have feedforward structures, consisting of only one hidden layer with locally tuned neurons and are fully interconnected to the output layer. The general architecture of a RBF ANN is illustrated in Fig. 6a. A schematic of the RBF ANN with *N* inputs and a scalar output is given in Fig. 6b. The input layer has, as in many other network models, no calculating power and serves only to distribute the input data among the hidden neurons. The hidden neurons show a non-linear transfer function which is derived from Gaussian bell curves (radial basis function units). The output neurons in turn have a linear transfer function which makes it possible to simply calculate the optimum weights associated with these neurons. With this architecture, the training process should be improved [19].

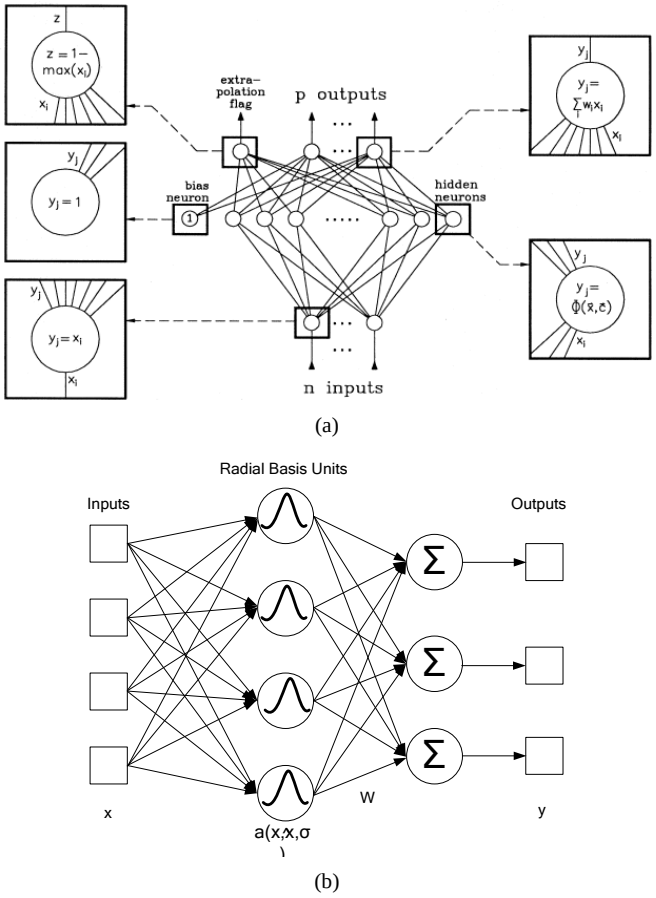

Fig. 6. RBF ANN: (a) Global architecture. (b) The adopted architecture.

There are *H* neurons in the ANN hidden layer. The transfer function used is similar to the Gaussian density function.

$$a_{hk} = \exp(-\left\|\hat{x}_h - x_k\right\|^2 / \sigma_h^2) \tag{3}$$

Where a_{hk} is the activation of the *h*th unit in the hidden layer given the input x_k. Each neuron is associated with N+1 parameters $\hat{x}$, N is the dimensional position of the center of the radial unit in the input space, and σ a distance scaling parameter which determines over what distance in the input space the unit will have a significant influence. The parameter σ has the same function as standard deviation in the standard normal probability distribution, although it is not estimated in the same way [19].

The connections in the second layer are weighted as usual in classical ANN. The ANN output is given by

$$y_m = \sum_{h=1}^{H} w_{mh} a_h \tag{4}$$

The training data set is formulated in the same way as for a backpropagation ANN. The target output vector *T* has a single "l" in the position corresponding to the correct class and zeroes elsewhere. The training is done by minimizing the same objective function

$$E(\hat{x}, \sigma, w) = \sum_{k=1}^{K} \left\| y_k - T_k \right\|^2 \tag{5}$$

A single procedure, analogous to backpropagation, to optimize the error function would be difficult. However, the problem of training can be decomposed quite naturally. The parameters for radial basis function units are determined in three steps: unit centers $\hat{x}$ computation, scaling parameters σ_h computation and finally computation of the ANN second layer weighted connections [19].

IV. Experimental Tests

A. Test Facility Description

Figure 7a describes the experimental setup. It is composed of two parts: a mechanical part that has a tacho-generator, a three-phase squirrel cage induction motor and a car alternator. The tacho-generator is a DC machine that generates 90 V at 3000 rpm. It is used to measure system the speed. It produces linear voltage between 2500 and 3000 rpm. The alternator is a three-phase synchronous machine with a regulator and a rectifier circuit that stabilize the output voltage at 12 VDC. The advantage of using a car alternator instead of DC generator is obtaining constant output voltage at various speeds. The induction motor could be identically loaded at different speeds.

Moreover, if the induction motor is supplied from the network, motor current will have time and space harmonic components as well as bearing fault sourced harmonics. This makes it harder to determine the bearing failure effect on the stator current and therefore complicates the fault detection process. For these reasons, the induction is fed by an alternator. By this way, supply harmonics effects are eliminated and only bearing failure effects could be observed on the stator current. Figure 7b is then given to illustrate the experimental test philosophy.

The induction motor, that is installed in a test jig, has the following rated parameters: 0.75 kW, 220/380 V, 1.95/3.4 A, 2780 rpm, 50 Hz, 2 poles, Y-connected. The induction motor has two 6204.2ZR type bearings.

From the bearing data sheet following parameters are obtained. The outside diameter is 47 mm and inside one is 20 mm. Assuming that the inner and the outer races have the same thickness gives the pitch diameter D_P = 31.85 mm. The bearing has eight balls (N = 8) with an approximate diameter of D_B = 12 mm and a contact angle of $\theta = 0^\circ$. These bearings are made to fail by drilling holes various radiuses with a diamond twist bit while controlling temperature by oil circulation in experiments. Some of the artificially deteriorated bearings are shown in Fig. 8.

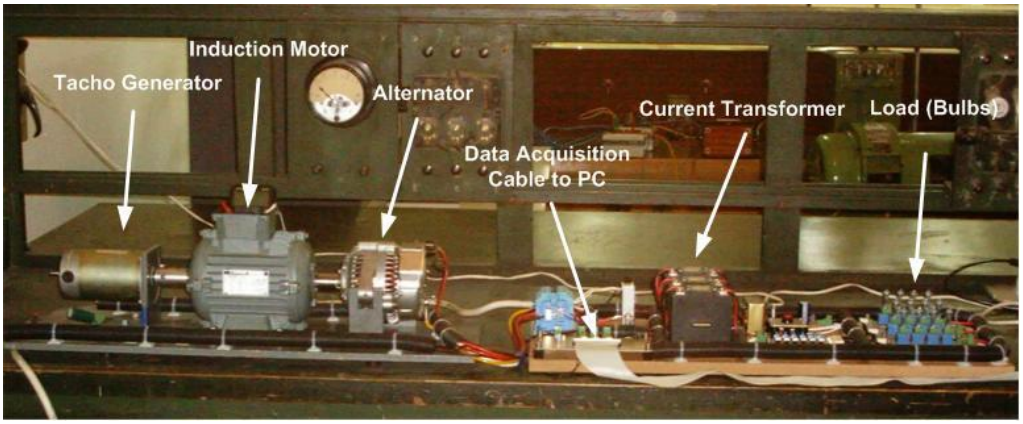

(a)

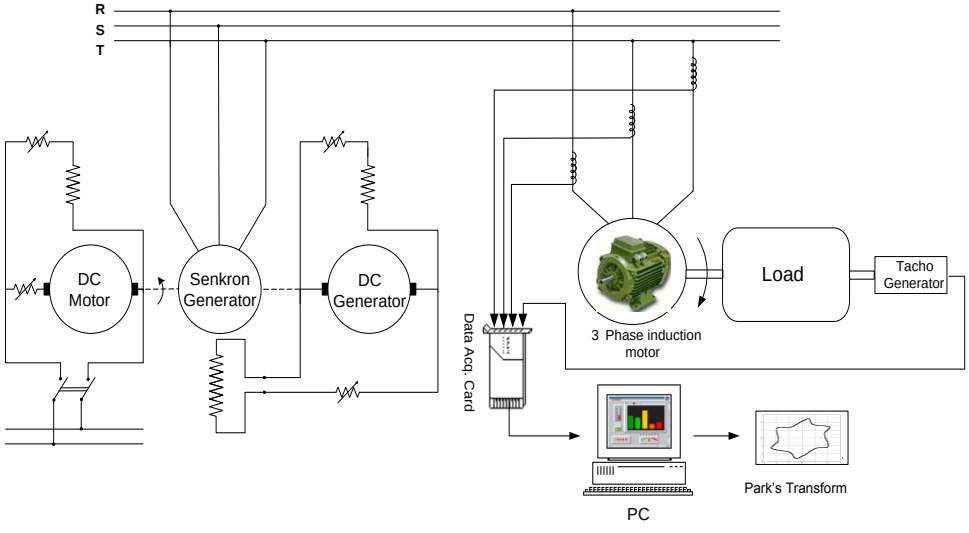

(b)

Fig. 7. Test facility.

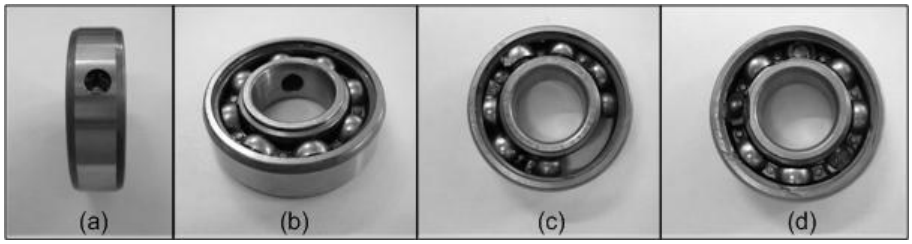

Fig. 8. Artificially deteriorated bearings: (a) outer race deterioration,(b) inner race deterioration, (c) cage deterioration, (d) ball deterioration.

B. Experimental Tests of the Proposed Approach

The fault detection and diagnosis process could be summarized as: the occurrence of a bearing failures manifest itself in the deformation of the current pattern corresponding to a healthy condition (*failure detection*). The deformation analysis will lead to the *failure diagnosis*.

Sampling frequency is chosen as 10 kHz. All the data obtained are used to compute stator *sD-sQ* and *D-Q* components to obtain *D-Q* patterns. The induction motor has been initially tested with healthy bearings in order to determine the reference current Park. Afterwards, it has been tested with the different artificially deteriorated bearings. These experiments are summarized by Fig. 9. It could be seen that bearing failures cause a clear deformation of the stator current *D–Q* trajectory. Moreover, an insight analysis of Fig. 9 leads to an obvious classification of bearing failure according to a specific deformation of the initial ellipse: this clearly show the diagnosis capability of the proposed Park transform.

The RBF ANN in then used o automate the fault detection process. The RBF network structure is realized and optimized (training and tests) using Matlab®. The RBF network has 400 input neurons, 50 hidden neurons and 2 output neurons.

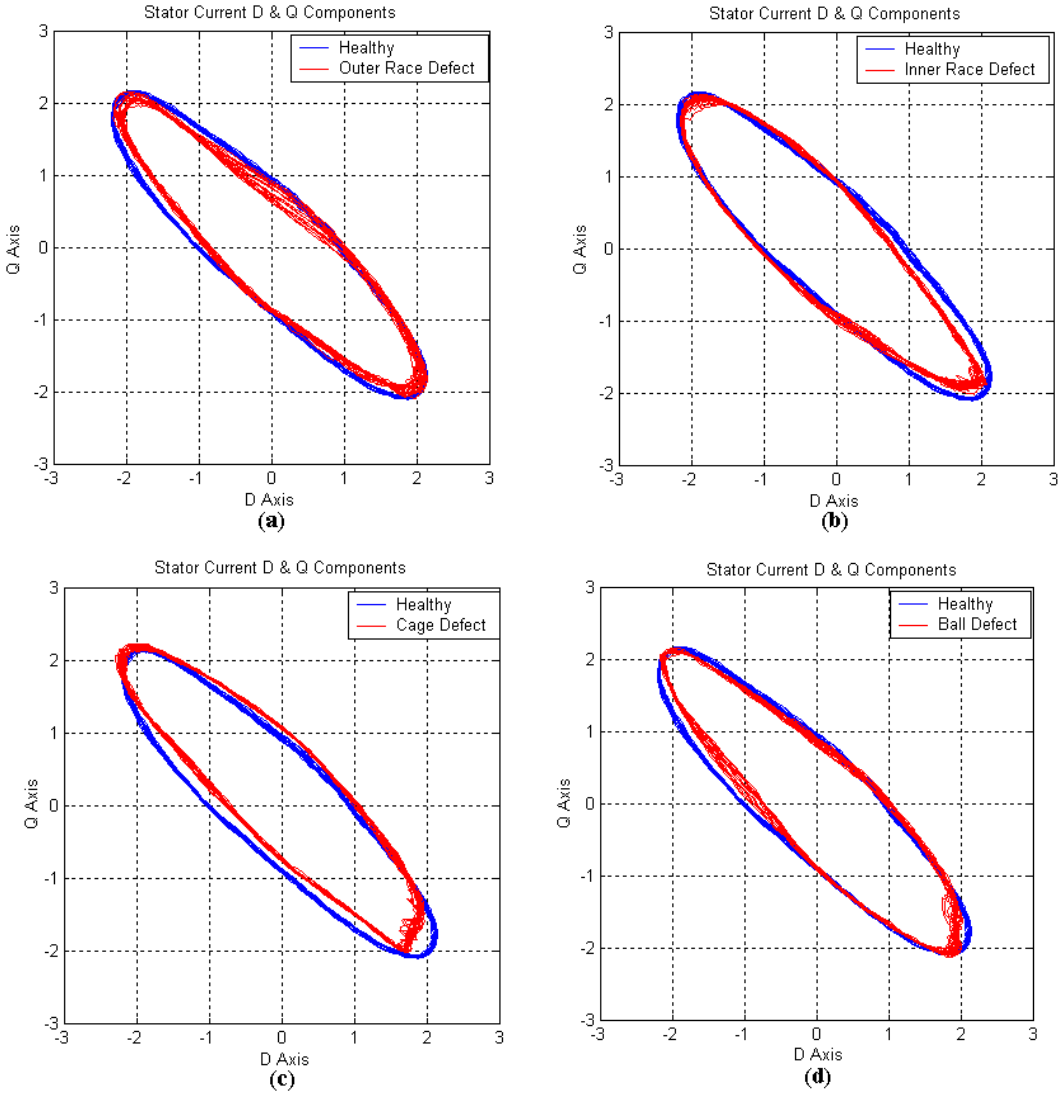

Fig. 9. Stator current *D–Q* components trajectory comparison: (a) Healthy and outer race defect, (b) Healthy and inner race defect, (c) Healthy and cage defect, (d) Healthy and ball defect.

The adopted structure is schematically shown in Figure 10. In this case, as the sampling frequency is 10 kHz (there are 200 samples in a period), we have 200 *D* and 200 *Q* stator current components in a period (20 msec). These components are the inputs of the network. For the ANN output side, if O_1 is active, it means that the induction motor is healthy. If O_2 is active, it means that the induction motor has bearing failures. It should be noticed that for test purposes, the scaling factor is manually chosen as 2.5.

The RBF ANN has been successfully trained, giving 100% correct prediction for the training data. When it was presented a set of Park patterns upon which it has not been trained, the RBF ANN guessed the bearing conditions with 96% accuracy. It should be noted that the testing performances have been evaluated using Chow approach [17].

V. Concluding Remarks and Perspectives

This paper has introduced a specific application of the Park transform for bearing failure detection and diagnosis in induction motors. This transform has been coupled to a RBF neural network to automate the detection and diagnosis process. What could be stated as a drawback of the proposed approach is that it requires the speed information and therefore a speed sensor. This could be justified by the importance of bearing failures detection as they account for approximately 50% of total failures in induction motors. Otherwise, sensorless fault detection and diagnosis should be performed as in [21], where the speed is estimated from the motor current rotor slot harmonic.

The generality of the proposed methodology has been experimentally tested on a 0.75-kW two-pole induction motor. Experimental tests have led to results with a level of accuracy of 96%, which is satisfactory and promising for an industrial application in the particular case of small induction motors.

To improve the proposed fault detection and diagnosis approach, experimental aspects should be carried out carefully as it was recently pointed out in [22]: *"When obtaining experimental data from bearings failed offline, the act of reassembling, remounting, and realigning the test machine significantly affects the stator current. If this phenomenon is not understood and acknowledged, it can have detrimental consequences when these data are used to develop or evaluate many bearing condition monitoring schemes"*.

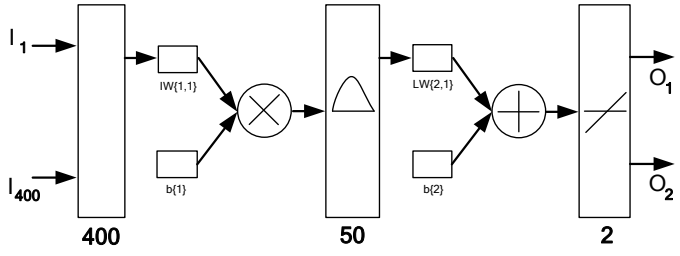

Fig. 10. Structure of the ANN used in fault detection

References

[1] M.E.H. Benbouzid et *al.*, "What stator current processing based technique to use for induction motor rotor faults diagnosis?," *IEEE Trans. Energy Conversion*, vol. 18, n°2, pp. 238-244, June 2003.

[2] O.V. Thorsen et *al.*, "Failure analysis for high-voltage induction motors in the petrochemical industry," *IEEE Trans. Industry Applications*, vol. 35, n°4, pp. 810-818, July-August 1999.

[3] J. Riddle, *Ball Bearing Maintenance*. Norman, OK: Univ. of Oklahoma Press, 1955.

[4] P. Eschmann et al., Ball and Roller Bearings: Their Theory, Design, and Application. K.G. Heyden: London, 1958

[5] T. Harris, *Rolling Bearing Analysis*. Wiley: New York, 2001.

[6] R.F. Schiferl et *al.*, "Bearing current remediation options," *IEEE Industry Applications Magazine*, vol. 10, n°4, pp.40-50, July-August 2004.

[7] N. Tandon et *al.*, "A review of the vibration and acoustic measurement methods for detection of defects in rolling element bearings," *Tribology International*, vol. 32, n°8, pp. 469–480, 1999.

[8] N. Tandon et *al.*, "A comparison of some condition monitoring techniques for the detection of defects in induction motor ball bearings," *Mechanical Systems and Signal Processing*, 2005.

[9] R.R. Schoen et *al.*, "Motor bearing damage detection using stator current monitoring", *IEEE Trans. Industry Applications*, vol. 31, nº 6, pp. 1274-1279, November-December 1995.

[10] A.M. Knight et *al.*, "Mechanical fault detection in a medium-sized induction motor using stator current monitoring," *IEEE Trans. Energy Conversion*, vol. 20, n°4, pp. 753-760, December 2005.

[11] B. Yazici et *al.*, "An adaptive statistical time-frequency method for detection of broken bars and bearing faults in motors using stator current," *IEEE Trans. Industrial Applications*, vol. 35, n°2, pp. 442–452, March-April 1999.

[12] L. Eren et *al.*, "Bearing damage detection via wavelet packet decomposition of the stator current" *IEEE Trans. Instrumentation and Measurement*, vol. 53, n°2, pp. 431-436, April 2004.

[13] B. Li et *al.*, "Neural-network based motor rolling bearing fault diagnosis," *IEEE Trans. Industrial Electronics*, vol. 47, n°5, pp. 1060–1068, October 2000.

[14] M.E.H. Benbouzid et *al.*, "Monitoring and diagnosis of induction motors electrical faults using a current Park's vector pattern learning approach," *IEEE Trans. Industry Applications*, vol. 36, n°3, pp. 730-735, May-June 2000.

[15] J.L.H. Silva et *al.*, "Bearing failures in three-phase induction motors by extended Park's vector approach" *in Proceedings of the IEEE IECON'05*, Raleigh, NC (USA), pp. 2591-2596, November 2005.

[16] M.E.H. Benbouzid et *al.*, "Induction motor stator faults diagnosis by a current Concordia pattern based fuzzy decision system," *IEEE Trans. Energy Conversion*, vol. 18, n°4, pp. 469-475, December 2003.

[17] M.Y Chow, Methodologies of Using Neural Network and Fuzzy Logic for Motor Incipient Fault Detection, Singapore: World Scientific, 1997.

[18] F. Filippetti et *al.*, "Recent developments of induction motor drives fault diagnosis using AI techniques," *IEEE Trans. Industrial Electronics*, vol. 47, n°5, pp. 994–1004, October 2000.

[19] J.A. Leonard et *al.*, "Radial basis function networks for classifying process faults," *IEEE Control Systems*, vol. 11, n° 3, pp. 31-38, 1991.

[20] S. Wu et *al.*, "Induction machine fault detection using SOM-based RBF neural networks," *IEEE Trans. Industrial Electronics*, vol. 51, n°1, pp. 183–194, February 2004.

[21] K. Kim et *al.*, "Sensorless fault diagnosis of induction motors," *IEEE Trans. Industrial Electronics*, vol. 50, n°5, pp. 1038–1051, October 2003.

[22] J.R. Stack et *al.*, "experimentally generating faults in rolling element bearings via shaft current," *IEEE Trans. Industry Applications*, vol. 41, n°1, pp. 25–29, January-February 2005.